

Molecular 3C approximation for the ionization of H₂ by positron impact

Á Benedek and R I Campeanu

Department of Physics and Astronomy, York University 4700 Keele Street, Toronto M3J 1P3, Canada

E-mail: campeanu@yorku.ca

Received 26 January 2007, in final form 13 March 2007

Published 30 March 2007

Online at stacks.iop.org/JPhysB/40/1589

Abstract

A molecular three-continuum approximation which was developed in the study of (e, 2e) collisions is applied for positron impact ionization of H₂. Our triple differential cross sections are compared with the experiment and with other theoretical results.

1. Introduction

Experimental triple differential cross sections (TDCS) for the ionization of H₂ by positrons have been obtained in a relative scale by Kövér and Laricchia (1998, 2001). These measurements focused on the electron capture to the continuum (ECC) phenomenon.

On the theoretical front most of the work was focused on obtaining TDCS for the ionization of H₂ by electron impact. The distorted wave Born approximation (DWBA) of Monzani *et al* (1999), the two-effective centre approximation (TEC) of Weck *et al* (2001) were followed by the molecular Brauner–Briggs–Klar (MBBK) model of Stia *et al* (2002). More recently, TDCS for the ionization of H₂ by electron impact were obtained by Gao *et al* (2006) using the distorted wave impulse approximation with orientation-averaged molecular orbitals (DWIAOA) and the molecular three-body distorted wave (M3DW) approximation.

From all these theoretical approximations only the Brauner–Briggs–Klar (BBK) model was applied to the ionization of H₂ by positrons (Fiol *et al* 2001, Berakdar 1998). The BBK model was applied originally for the ionization of the atomic hydrogen by electron impact. Both papers on the ionization of H₂ by positrons assumed that the target is comprised of two non-interacting hydrogen atoms, and therefore we shall refer to this model as ‘twice BBK’ or 2BBK. The theoretical 2BBK TDCS were in good agreement with the measurements for 100 eV positrons. However, for 50 eV positrons the experimental ECC peak appeared at an energy which was about 1.6 eV lower than the energy of the theoretical ECC peak obtained by Fiol *et al* (2001) after the convolution with the experimental angular and energy resolution. Recent experimental work (Arcidiacono *et al* 2005) confirmed the accuracy of the experimental

data and demonstrated the need for further calculations on this problem. It is interesting to note that the classical trajectory Monte Carlo (CTMC) method (Fiol and Olson 2002) gives results which are in better agreement with the experiment at 50 eV than at 100 eV. The CTMC calculations showed that at 50 eV there is a strong correlation between the momenta of the positron and of the residual ion.

In this paper, we shall use the MBBK model of Stia *et al* (2002) for the positron impact ionization of H_2 . MBBK used the three-continuum (3C) approximation introduced in BBK by Brauner *et al* (1989). In the 3C approximation, Coulomb functions represent the interaction between the three particles of the final state of the ionizations system (the scattered positron, ejected electron and residual ion). In addition, MBBK also uses a two-effective-centre approach and Wang's (1928) H_2 molecular representation. Our work differs from that of Stia *et al* (2002) not only because it refers to a positron projectile but also in the numerical methods employed.

2. Theory

The triple differential cross section for the ionization of a molecule by positron impact may be written as

$$\frac{d^3\sigma}{d\hat{\mathbf{k}}_s d\hat{\mathbf{k}}_e dE_e} = 2 \frac{1}{4\pi} (2\pi)^4 \frac{k_e k_s}{k_i} \int d\Omega_\rho |t_{fi}(\boldsymbol{\rho}_0)|^2, \quad (1)$$

where E_e is the energy of the ejected electron, k_i is the incident positron momentum, k_e , k_s and $\hat{\mathbf{k}}_e$, $\hat{\mathbf{k}}_s$ stand for the size and direction of the momenta of the ejected electron and scattered positron, respectively. In equation (1) $\boldsymbol{\rho}_0$ stands for the equilibrium internuclear vector of the molecular target. The transition matrix element can be written as

$$t_{fi} = \langle \Psi_f^-(\boldsymbol{\rho}_0, \mathbf{R}, \mathbf{r}_1, \mathbf{r}_2) | V_i | \Psi_i(\boldsymbol{\rho}_0, \mathbf{R}, \mathbf{r}_1, \mathbf{r}_2) \rangle, \quad (2)$$

where Ψ_i is the wavefunction in the initial state, Ψ_f^- is the final state wavefunction with correct asymptotic conditions described in Brauner *et al* (1989). Coordinates are described in the laboratory system and they are sketched in figure 1. V_i is the perturbation in the entrance channel, given by

$$V_i = \frac{1}{R_a} + \frac{1}{R_b} - \frac{1}{r_{1p}} - \frac{1}{r_{2p}}. \quad (3)$$

The incident state wavefunction is

$$\Psi_i = \frac{e^{i\mathbf{k}_i \cdot \mathbf{R}}}{(2\pi)^{3/2}} \Phi_i(\boldsymbol{\rho}_0, \mathbf{r}_1, \mathbf{r}_2), \quad (4)$$

where Φ_i describes the initial molecular bound state which is represented by the Heitler–London-type wavefunction proposed by Wang (1928),

$$\Phi_i(\boldsymbol{\rho}_0, \mathbf{r}_1, \mathbf{r}_2) = N(\boldsymbol{\rho}_0) (e^{-\alpha^* r_{1a}} e^{-\alpha^* r_{2b}} + e^{-\alpha^* r_{1b}} e^{-\alpha^* r_{2a}}), \quad (5)$$

with $\alpha^* = 1.166$, $\rho_0 = 1.406$ and $N(\boldsymbol{\rho}_0)$ is the normalization function. The final state wavefunction is

$$\Psi_f^- = \frac{e^{i\mathbf{k}_f \cdot \mathbf{R}}}{(2\pi)^{3/2}} \Phi_f(\boldsymbol{\rho}_0, \mathbf{r}_2) \xi_c, \quad (6)$$

where Φ_f is the bound state of the residual H_2^+ molecular ion represented by a simple combination of atomic orbitals

$$\Phi_f(\boldsymbol{\rho}_0, \mathbf{r}_2) = N_f(\boldsymbol{\rho}_0) (e^{-\alpha r_{2a}} + e^{-\alpha r_{2b}}), \quad (7)$$

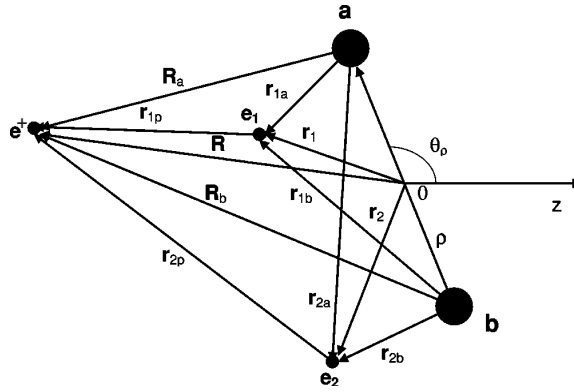


Figure 1. Coordinates used in the text.

with $N_f(\rho_0)$ being the normalization factor and $\alpha = 1.3918$ is the variational parameter. The function ξ_c in equation (6) was chosen as in the BBK approximation

$$\xi_c = \frac{e^{i\mathbf{k}_e \cdot \mathbf{r}_1}}{(2\pi)^{3/2}} C(\mathbf{k}_e, \mathbf{r}_{1j}, \gamma_e) C(\mathbf{k}_s, \mathbf{R}_j, \gamma_s) C(\mathbf{k}_{1p}, \mathbf{r}_{1p}, \gamma_{ep}), \quad (8)$$

where $j = a$ or b . The function corresponding to $j = a(b)$ is used when the exponential term $e^{-\alpha^* r_{1a}}$ ($e^{-\alpha^* r_{1b}}$) is present in the matrix transition element given by equation (2). This is in agreement with the assumption that when the active electron is ionized from the proximities of one molecular centre, the passive electron completely screens the other nucleus. The Coulomb factor $C(\mathbf{k}, \mathbf{r}, \gamma)$ has the form

$$C(\mathbf{k}, \mathbf{r}, \gamma) = \Gamma(1 - i\gamma) e^{-\pi\gamma/2} {}_1F_1(i\gamma; 1; -i(kr + \mathbf{k}\mathbf{r})). \quad (9)$$

The Sommerfeld parameters γ_e , γ_s and γ_{ep} are given by

$$\gamma_s = 1/k_s, \quad \gamma_e = -1/k_e, \quad \gamma_{ep} = \frac{-1}{2k_{1p}}, \quad (10)$$

where $\mathbf{k}_{1p} = \frac{1}{2}(\mathbf{k}_s - \mathbf{k}_e)$ is the momentum conjugate to \mathbf{r}_{1p} . In equation (6) it is supposed that electron 1 is ionized. The possibility that electron 2 is ionized is taken into account by means of the factor 2 in equation (1).

The paper by Stia *et al* (2002) shows the detailed analytical work producing the transition matrix element and the integration over all possible molecular orientations. Like in the work of Fiol *et al* (2001) we reduced the resulting six-dimensional integrals to three-dimensional integrals using Nordsieck integrals (Nordsieck 1954). The numerical integration of the three-dimensional integrals presents a challenge because of sharp changes in the integrand. We applied a three-dimensional adaptive Simpson integration method to obtain these integrals.

3. Results and discussion

In figures 2 and 3 we present our results for 50 and 100 eV impact energies and zero ejected and scattering angles. Our MBBK triple differential cross sections are compared with the ‘twice BBK’ results of Fiol *et al* (2001). The results of Berakdar (1998) for 100 eV are identical to those of Fiol *et al* (2001). Both figures show that the molecular target representation (MBBK) results are similar to the 2BBK results. The only disagreement appears in figure 3,

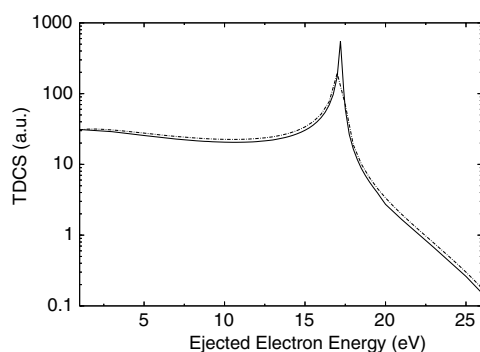


Figure 2. TDCS as a function of the ejected electron energy for 50 eV impact energy. Both emerging particles are detected in the forward direction. MBBK results for positron impact are represented by the full line, and 2BBK results of Fiol *et al* (2001) by the dot-dashed line.

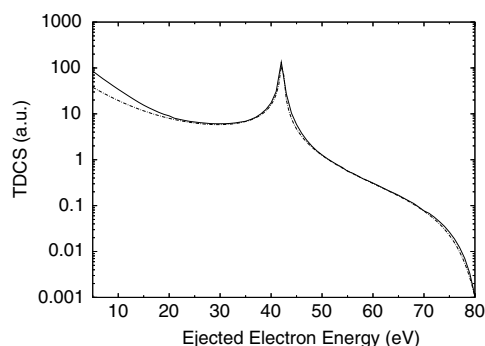


Figure 3. Same as in figure 2 but for 100 eV impact energy.

where for ejected electron energies below 20 eV the MBBK results are higher than the 2BBK results.

A comparison with experiment can be done only after the convolution with the experimental angular and energy resolution of Kövér *et al* (1998, 2001). In our work, we used two different sets of resolution data for the 50 eV and 100 eV cases. In the work of Fiol *et al* (2001) the same resolution data were used for both cases. By convolution the position of the peak shifts to a lower ejected electron value. For instance for the 50 eV case the peak position shifts from 17.3 eV (see figure 2) to 16.5 eV.

Figure 4 compares our convoluted MBBK data for 50 eV impact energy with the experimental data and with the 2BBK data of Fiol *et al* (2001). Two adjustments were made to facilitate this comparison. First, both theoretical data sets were shifted by 1.6 eV towards lower ejected electron energies to have their peaks for the same energy as the experiment. Second, the experimental data, which were produced in a relative scale, were made to match our peak size. Figure 4 shows that our MBBK model is in better agreement with the experiment than the 2BBK model of Fiol *et al* (2001). However, the fact that this agreement was obtained with a 1.6 eV shift of our data illustrates that our MBBK model is unable to correctly reproduce the experiment. Figure 4 shows that the accurate representation of the molecular target does not produce an EEC peak at the correct ejected electron energy. The

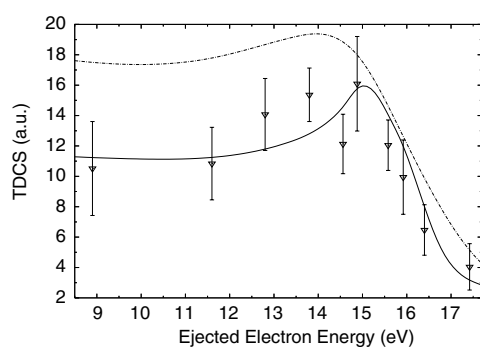


Figure 4. Convolved TDCS as a function of the ejected electron energy for 50 eV impact energy. Both emerging particles are detected in the forward direction. MBBK results for positron impact are represented by full line, 2BBK results of Fiol *et al* (2001) by the dot-dashed line and experimental data by symbols. The theoretical data were shifted by 1.6 eV to fit the position of the experimental peak.

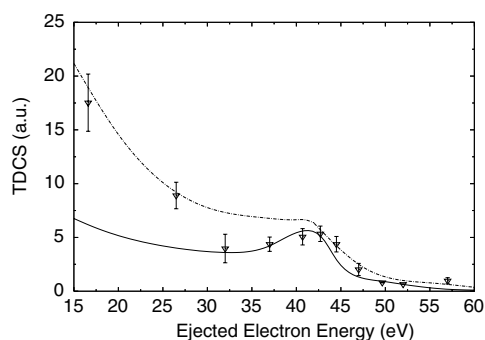


Figure 5. Same as in figure 4 but for 100 eV impact energy, where no shift of the theoretical data is needed.

most likely phenomenon responsible for the shift of the theoretical peak is the interaction between the direct ionization and the positronium formation channels, as suggested by J Walters (see the paper by Arcidiacono *et al* (2005)). For 50 eV impact energy the positronium formation is very important and will influence significantly the ionization process. A much more sophisticated theoretical model should contain both the ionization and the positronium formation channels.

In figure 5, we present the convolved theoretical data compared with the experiment for 100 eV impact energy. In this case both theories produce the EEC peak at the same ejected electron energy as the experiment. Our MBBK data seem to be in better agreement with the experiment for ejected electron energies above 30 eV, while for lower energies the 2BBK data agree better with the two experimental points. The 2BBK results of Berakdar (1998) seem to agree with those of Fiol *et al* (2001) except for very small ejected electron energies where they are below the experimental points.

Both figures 4 and 5 show that the differences between MBBK and 2BBK models are significantly larger in the convolved TDCS than in the unconvoluted data. These differences are explained in part by the fact that the convolution work includes contributions from non-zero

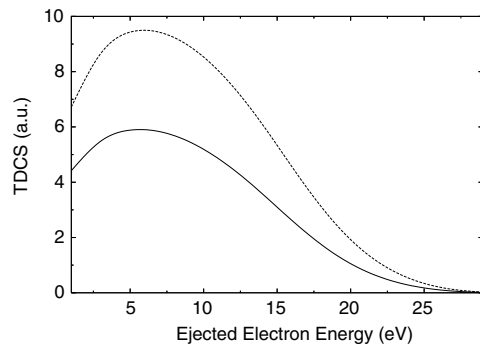


Figure 6. TDCS as a function of the ejected electron energy for 50 eV impact energy and for positron and electron angles $(-15^\circ, -4^\circ)$ and $(12^\circ, 4^\circ)$ respectively. We used a solid line for present MBBK and a dashed line for our present 'twice BBK'.

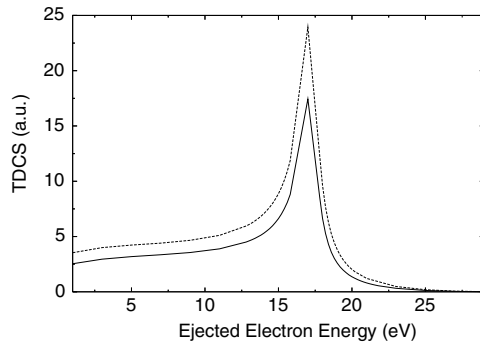


Figure 7. Same as figure 6 but for positron and electron angles $(12^\circ, 4^\circ)$ and $(12^\circ, -4^\circ)$ respectively.

angles cases, and also by the fact that our numerical work is different from that of Fiol *et al* (2001). Figures 6 and 7 illustrate the differences between MBBK and 2BBK for some non-zero angles used in the convolution work. Figure 6 shows the unconvoluted TDCS obtained with MBBK and our 2BBK models for 50 eV impact energy and for positron and electron angles $(\Theta_p = -15^\circ, \Phi_p = -4^\circ)$ and $(\Theta_e = 12^\circ, \Phi_e = 4^\circ)$ respectively. Figure 7 shows the unconvoluted TDCS obtained with MBBK and our 2BBK models for 50 eV impact energy and for positron and electron angles $(\Theta_p = 12^\circ, \Phi_p = 4^\circ)$ and $(\Theta_e = 12^\circ, \Phi_e = -4^\circ)$ respectively. Unfortunately, there are no experimental TDCS data for positron impact ionization of H_2 at other angles to verify that MBBK produces better data than the 2BBK model. The paper of Stia *et al* (2002) demonstrates that indeed this is the case in the electron impact case.

Another case of interest for which no experimental data are available is shown in figure 8. This figure shows the variation of the TDCS with the ejection angle for 100 eV incident positrons, for 19 eV ejected electrons and when the positrons and electrons are moving in the same direction. In this graph a pronounced minimum occurs at an angle of 22.5° . Della Picca *et al* (2005) interpreted this minimum as corresponding to an ejected electron lying in the saddle-point of the scattered positron and residual ion potentials, when it

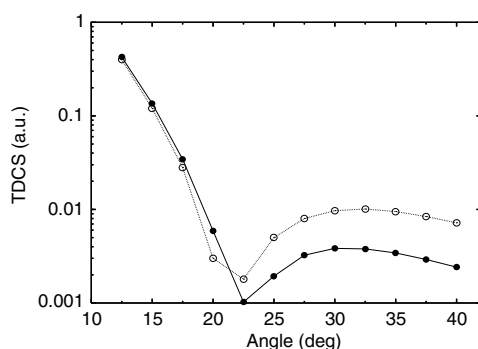


Figure 8. TDCS as a function of the particles final direction. $\Theta_e = \Theta_s$, 100 eV impact energy, and $E_e = 19$ eV. Full circles represent our MBBK results, while the open circles represent the 2BBK results of Della Picca *et al* (2005).

moves free-of-forces. Our MBBK results are a bit lower than the 2BBK data of Della Picca *et al* (2005) for angles above 22 degrees.

4. Conclusions

Our work is an attempt to improve the theory used to calculate TDCS for positron impact ionization of H₂. We show that improving the representation of the H₂ target improves the agreement between a 3C model data and the experiment. The only case where the 2BBK model seems to be in better agreement with the experiment is the 100 eV impact case, for ejected electron energies below 30 eV.

We find that our 50 eV ECC peak is shifted relative to the experimental peak by the same energy as in the 2BBK model. This leads us to conclude that the shift is most likely due to the absence in the theory of the interaction between the ionization and positronium formation channels. The fact that the shift occurs for 50 eV and not for 100 eV positrons most likely corresponds to the fact that positronium formation is very significant for 50 eV and not significant for 100 eV positrons.

Our work also suggests that new experimental TDCS are needed particularly for non-zero positron scattering and ejected electrons angles. These experiments can fully verify the accuracy of the MBBK model, which in those cases is very different from the 2BBK model.

Acknowledgments

This research was supported by a grant from the Natural Sciences and Engineering Research Council of Canada. The authors want to thank Dr J Fiol for several useful discussions related to this project, Dr O Fojon for sending his tabulated electron impact MBBK results (which were used to test our program), and Dr G Laricchia for sending the angular and energy resolution of her TDCS measurements.

References

- Arcidiacono C, Kóvér Á and Laricchia G 2005 *Phys. Rev. Lett.* **95** 223202
 Berakdar J 1998 *Phys. Rev. Lett.* **81** 1393
 Brauner M, Briggs J S and Klar H 1989 *J. Phys. B: At. Mol. Opt. Phys.* **22** 2265

- Fiol J, Rodriguez V D and Barrachina R O 2001 *J. Phys. B: At. Mol. Opt. Phys.* **34** 933
- Fiol J and Olson R 2002 *J. Phys. B: At. Mol. Opt. Phys.* **35** 1173
- Gao J, Madison D H and Peacher J L 2006 *J. Phys. B: At. Mol. Opt. Phys.* **39** 1275
- Kövér Á and Laricchia G 1998 *Phys. Rev. Lett.* **80** 5309
- Kövér Á, Paludan K and Laricchia G 2001 *J. Phys. B: At. Mol. Opt. Phys.* **34** L219
- Monzani A L, Machado L E, Lee M T and Machado A M 1999 *Phys. Rev. A* **60** R21
- Nordsieck A 1954 *Phys. Rev.* **93** 785
- Della Picca R, Fiol J and Barrachina R O 2005 *Nucl. Instrum. Methods Phys. Res.* **233** 270
- Stia C R, Fojon O A, Weck P K, Hanssen J, Joulakian B and Rivarola R D 2002 *Phys. Rev. A* **66** 052709
- Wang S C 1928 *Phys. Rev.* **39** 579
- Weck P, Fojon O A, Hanssen J, Joulakian B and Rivarola R D 2001 *Phys. Rev. A* **63** 042709